© 2017. Published by The Company of Biologists Ltd | Development (2017) 144, 3946-3956 doi:10.1242/dev.155507

STEM CELLS AND REGENERATION

RESEARCH ARTICLE

Distinct regenerative potential of trunk and appendages of *Drosophila* mediated by JNK signalling

Raquel Martín, Noelia Pinal and Ginés Morata*

ABSTRACT

The *Drosophila* body comprises a central part, the trunk, and outgrowths of the trunk, the appendages. Much is known about appendage regeneration, but little about the trunk. As the wing imaginal disc contains a trunk component, the notum, and a wing appendage, we have investigated the response to ablation of these two components. We find that, in contrast with the strong regenerative response of the wing, the notum does not regenerate. Nevertheless, the elimination of the wing primordium elicits a proliferative response of notum cells, but they do not regenerate wing; they form a notum duplicate. Conversely, the wing cells cannot regenerate an ablated notum; they overproliferate and generate a hinge overgrowth. These results suggest that trunk and appendages cannot be reprogrammed to generate each other. Our experiments demonstrate that the proliferative response is mediated by JNK signalling from dying cells, but JNK functions differently in the trunk and the appendages, which may explain their distinct regenerative potential.

KEY WORDS: *Drosophila*, Wing disc, Regeneration, Trunk, Appendages, JNK

INTRODUCTION

Regeneration is a widespread phenomenon that has been observed in many different animal groups (reviewed by Tanaka and Reddien, 2011); it refers to the response process triggered by injury or mutilation of organs or tissues that aims to reconstruct the damaged structure. Principal factors in regeneration are the induction of additional cell proliferation and the reprogramming of the resident cells that are necessary to rebuild the lost structures.

Experimental analysis in organisms with high regenerative potential is hampered by the limited number of genetic tools available. In contrast, the sophisticated genetic technology of *Drosophila* permits genetic manipulations not possible in other model organisms. A large body of classical studies described the regenerative capacity of the imaginal discs (the precursors of the adult skeleton). The experiments consisted of transplantation of fragments of imaginal discs into adult female hosts and the subsequent study of how those fragments regenerate missing parts (Hadorn and Buck, 1962; Nöthiger and Schubiger, 1966; Schubiger, 1971; Haynie and Bryant, 1976; reviewed by Worley et al., 2012). These experiments demonstrated that the wing and leg imaginal discs possess high regenerative potential, as some disc fragments were able to rebuild the whole discs. This method, however, had some limitations: it involved *in vivo* culture in heterologous medium and also relied on cutting disc fragments by hand under the dissecting microscope, which often resulted in imprecision in the size and shape of the fragments to test.

More recently, the development of new methods has allowed a more reliable and rigorous approach to study regeneration. The Gal4/UAS/Gal80^{TS} and other binary systems allow targeted ablation of well-defined body regions in time- and stage-dependent manners and the subsequent study of the regenerative response (Smith-Bolton et al., 2009; Bergantiños et al., 2010; Sun and Irvine, 2011; Herrera et al., 2013). Those studies have been focused on the wing disc and particularly the wing pouch, the region that corresponds to the appendage part of the wing disc.

The *Drosophila* body comprises two major parts: the body trunk and the appendages. The former constitutes the greater part of the body, whereas the appendages appear as additional structures that may have originated as outgrowths of the trunk. Moreover, their developmental processes are very different from those of the trunk. For example, in the case of the wing disc, the spatial positioning and function of major patterning genes such as *hedgehog* (*hh*), *decapentaplegic* (*dpp*) and *wingless* (*wg*) are different in the trunk region and the appendage; they induce different targets and their overexpression has different developmental consequences (reviewed by Morata and Sánchez-Herrero, 1999). Moreover, the function of Hox genes in the wing and haltere discs differs in trunk and appendages; in the former the specificity of Hox function requires critically the concourse of the Homothorax/Extradenticle (Hth/Exd) proteins, which are not active in the appendages. These distinct developmental features may also result in different regenerative responses to damage.

The wing disc is a convenient system with which to study differences between trunk and appendages because it contains a well-delimited trunk region, termed notum (the thoracic part), and an appendage region, which includes the wing pouch and the hinge (Fig. 1E). Recent reports have described the regeneration capacity of the appendage region (Smith-Bolton et al., 2009; Bergantiños et al., 2010; Sun and Irvine, 2011; Herrera et al., 2013) and found that it possesses strong regenerative potential. However, in these studies, the regeneration potential of the notum was not investigated.

Here, we use the wing disc to analyse the response to ablation of different regions of the prospective notum and wing. We find that, in contrast to the appendage regions, the notum shows very limited regenerative response. We also describe the response of notum cells to elimination of the entire wing primordium and that of the wing cells to massive apoptosis of the notum precursors. In the first case, the notum cells acquire a high proliferative rate, but are unable to regenerate a wing; they form instead a notum duplicate. In the second case, the wing cells close to the notum also overproliferate, but they do not regenerate a notum, they produce a wing outgrowth. In both cases, Jun-N terminal kinase (JNK) signalling emanating from dying cells is responsible for the increase in cell proliferation. Observations of the haltere disc indicate that the regenerative

Centro de Biología Molecular CSIC-UAM, Universidad Autónoma de Madrid, Madrid 28049, Spain.

*Author for correspondence (gmorata@cbm.csic.es)

G.M., 0000-0003-3274-5173

Received 29 May 2017; Accepted 11 September 2017

Development (2017) 144, 3946-3956 doi:10.1242/dev.155507

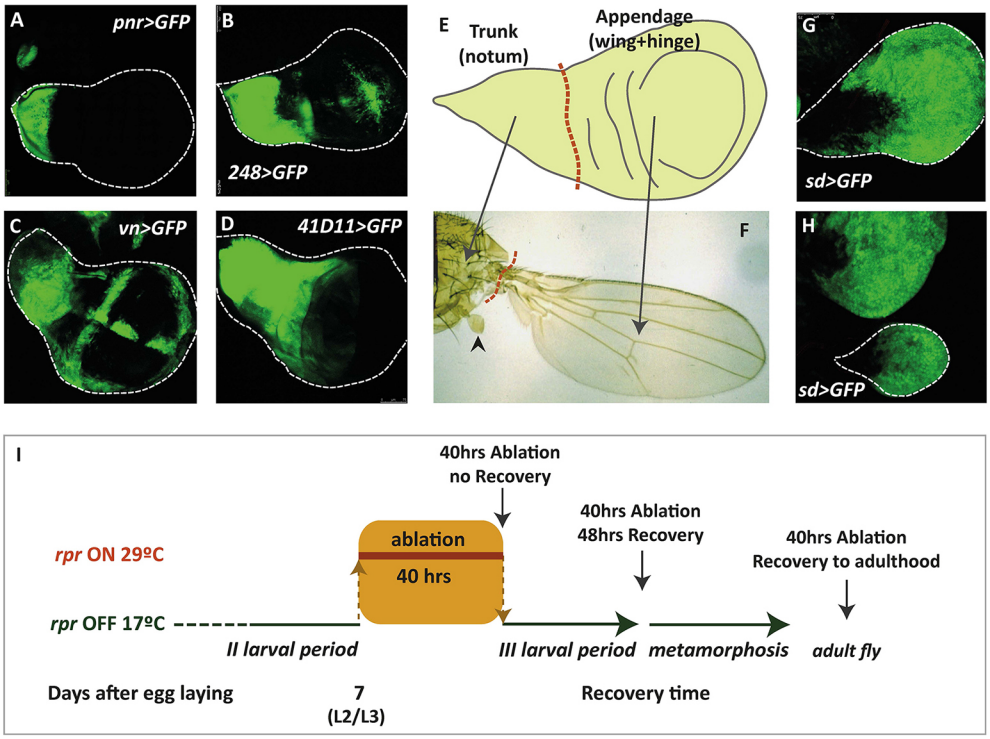

Fig. 1. Different Gal4 drivers used and general design of the experiments. (A-D) Notum domains defined (with UAS-GFP) by the *pnr-Gal4* (A), *248-Gal4* (B), *vn-Gal4* (C) and *4D11-Gal4* (D) lines. (E) Scheme of a mature wing disc; the dotted red line separates the notum and wing appendage components. (F) Adult derivatives of the wing disc, notum and wing appendage. The haltere appendage is indicated by an arrowhead. (G,H) Expression domain defined by the *sd-Gal4* driver in third instar wing (G) and haltere discs (H). The Sd domains are similar in both discs. (I) The scheme illustrates the standard ablation procedure. Larvae of the *X-Gal4>UAS-rpr Gal80^{TS}* genotype are kept at 17°C until day 7 after fertilisation and then shifted to 29°C for 40 h to allow unrestricted expression of *rpr* in the region defined by the Gal4 line. A shift back to 17°C stops ablation. Imaginal discs are fixed (vertical arrows) at the end of the ablation time, after 48 h of recovery or after recovery to adulthood.

response of the trunk region (metanotum) and appendage (haltere) mimics that of the homologous regions in the wing disc.

Our results indicate that, even though they are parts of the same imaginal disc, *Drosophila* trunk and the appendages become developmentally isolated from each. Our results also highlight the involvement of the JNK pathway in generating the additional cell proliferation required for the regeneration process. They also suggest that the different regenerative potential of the notum and wing may be due to differential function of JNK, for we show that forcing JNK activity has different effects in the notum and in the wing.

RESULTS

Regenerative response of the notum to the ablation of the Pnr, Vein and 248 domains

To study the response to damage of defined regions within the notum, we forced expression of the pro-apoptotic gene *reaper* (*rpr*) driven by the *pnr-Gal4*, *vein-Gal4* or *248-Gal4* lines (see Materials and Methods). The expression of the Pnr line defines the medial region of the notum and the Vein and 248 lines cover most of the notum, except the more medial region (Fig. 1A-C).

In the Pnr experiments, after 40 h of *rpr* activity, the domain was remarkably reduced and only a few *pnr-GFP* cells were detected, most of which were in apoptosis, as indicated by Dcp-1 staining (Fig. 2B,B′). Moreover, the expression of the notum marker Eyegone (Eyg) (Aldaz et al., 2003) was also significantly reduced in the ablated discs (Fig. 2D,D′). Staining with the anti-Wg antibody shows the thoracic Wg stripe just in the proximal border of the notum region (Fig. 2D,D″), whereas in control discs it occupies a more central position, at the border of the normal Pnr domain (Fig. 2C,C″). It indicates the elimination of most of the Pnr domain. After 48 h of recovery, the damaged discs were not capable of reconstructing the part of the Eyg territory lost during ablation; the Eyg domain remains reduced in the proximal region (Fig. 2E,E′). Moreover, the Wg stripe remains localised in the proximal border of the ablated disc (Fig. 2E,E″). Furthermore, all the *pnr>rpr* adult flies (n=30) that emerge after ablation show an abnormal thorax lacking the medial region (Fig. 2G), precisely the Pnr domain in the adult thorax (Calleja et al., 2000) in wild-type flies (Fig. 2F).

We also assayed cell proliferation levels in *pnr>rpr* discs after ablation and did not observe any significant difference in EdU label in the areas close to the ablated Pnr domain (Fig. 2H-I′ and Fig. S3A,B,D). These results indicate that the Pnr domain has little or no capacity to regenerate after ablation.

The results of the ablation of the Vein domain also indicate a similar conclusion. At the time we initiate the ablation, the Vein domain covers most of the notum (Fig. S1A). After the regular cell killing protocol, the Vein domain fails to regenerate. Even after 48 h of recovery the notum remains vestigial (Fig. S1C). This lack of regeneration is also visualised by Eyg staining, which is much reduced in comparison with the wild type, and also by the absence of significant proliferative stimulus in the areas around the ablated region (Fig. S1E,E′). Similar results were obtained by forcing *rpr* activity in the 248 domain, which results in wing discs that lack the corresponding region even after 48 h of recovery (Fig. S1G-I′) and do not show a significant proliferative response to the ablation (Fig. S1J-J″). Putting together the results obtained after ablation of the Pnr, Vein and 248 domains, the general conclusion is that the notum possesses very limited regenerative capacity.

Regenerative response to ablation of the wing and haltere precursors

In the following experiments, we analyse in the wing and haltere discs the response to the ablation of the entire appendage regions. These discs form the dorsal cuticular structures corresponding to the second and third thoracic segments. We have used the *sd-Gal4* line as driver and *UAS-rpr* and *UAS-hid* as pro-apoptotic vectors. The Sd expression domain covers homologous regions in the appendage part in both discs (Fig. 1G,H). In these experiments, in addition to targeting the domain for ablation with either *rpr* or *hid*, we have traced the cell lineage of the targeted area using a *UAS-Flp act>stop>lacZ* cassette combination (see Materials and Methods).

Development (2017) 144, 3946-3956 doi:10.1242/dev.155507

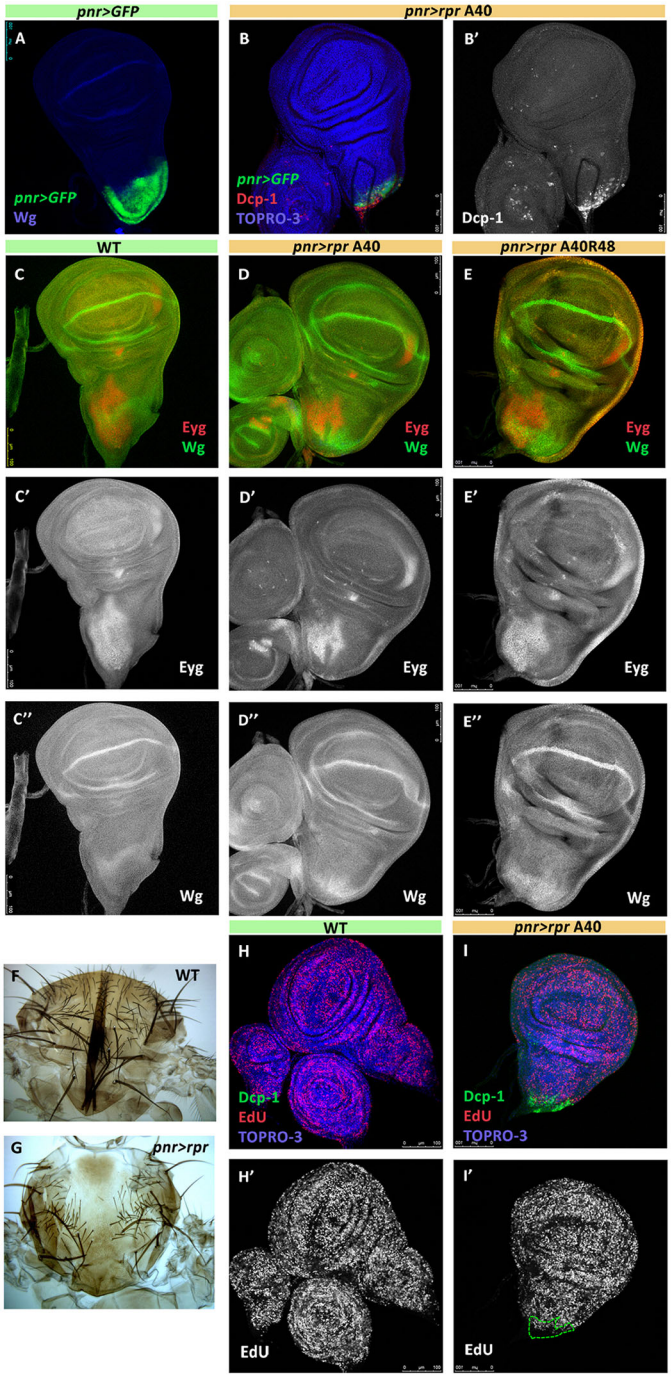

Fig. 2. Ablation of the Pnr domain. The Pnr domain covers approximately the proximal region of the notum, as indicated by GFP staining of *pnr-Gal4>UAS-GFP* discs (A). After 40 h of *rpr* activity, it is largely eliminated (B) and most of the remaining cells are dying, as indicated by the label of Dcp-1 (B,B′) (*n*=20). (C-C″) The expression of the notum markers Eyegone (Eyg) and Wingless (Wg) in the wild-type disc. Eyg covers most of the anterior notum (C′), whereas Wg is expressed in a longitudinal stripe in the middle of the notum (C″). (D-D″) The distribution of Eyg (red) and Wg (green) immediately after 40 h ablation (*n*=22). (E-E″) The distribution of Eyg and Wg after 40 h of ablation and 48 h of recovery (*n*=16), indicating that the ablated Pnr domain has not recovered. (F,G) Adult phenotype of *pnr>rpr* flies (G), in which the Pnr region is lacking (compare with wild type in F) (*n*=30 flies). (H-I′) EdU staining (red) in control and in ablated disc after 40 h of ablation (*n*=29). (Dcp-1, green). The dashed green line delimits the region expressing Dcp-1 in I′. A40 refers to discs fixed after 40 h of ablation and A40R48 refers to discs fixed 48 h after the end of the ablation.

We first describe the results obtained with *rpr* as pro-apoptotic agent. Wing discs from *sd>rpr* larvae are grossly altered after 40 h of *rpr* activity. They are very small and their morphology indicates that the regions corresponding to the wing pouch and hinge are lacking, except for a small group of cells with intense Dcp1 label close to the notum region (Fig. 3B). In effect, the treatment with *UAS-rpr* for 40 h amounts to a physical amputation of the Sd domain.

Discs allowed to recover for 48 h after ablation are still abnormal; they are small and show no sign of regeneration of wing structures (Fig. 3C). Instead, their morphology and the distribution of the Wg and Eyg proteins (Fig. 3F,G) suggest a duplication of notum patterns, which is especially clear in the case of the Wg stripe (Fig. 3G). Definitive proof of the duplication process is that the great majority of flies (270 out of 300 flies examined) that emerge in this experiment presented duplicated nota in mirror-image fashion (Fig. 3D).

The results in the haltere disc mimic in every aspect those found in the wing disc. After ablation it becomes very small and does not regenerate the appendage part after recovery. The flies that emerge lack the haltere appendage, although the response of the metanotum is hard to describe due to lack of morphological landmarks. Nevertheless, in mature haltere discs we observe a mirror-image disposition of the Wg stripe (Fig. 3H), clearly pointing to a duplication of the metanotum.

An important issue was to determine the origin of the cells that form the duplicated trunk structure. Duplicated notum structures have been reported to be associated with the loss of *wg* function in the wing primordium (Ng et al., 1996; Morata and Lawrence, 1977); the lack of *wg* activity causes the cells of the wing primordium to acquire notum fate. In our experiments the wing primordium is effectively eliminated by *rpr* activity; thus, we expected that the duplicate notum should derive from cells of the original notum. This issue was addressed by tracing the lineage of the wing territory subjected to ablation by using a *UAS-Flp* transgene in combination with the *act>stop>lacZ* cassette. This cassette recombines in *sd-Gal4*-expressing cells, thus generating multiple *lacZ*-expressing clones that are marked by β-galactosidase (β-gal) activity. In controls, all cells of the Sd territory were marked with β-gal (Fig. 3I, I′). In sharp contrast, *sd>rpr* discs subjected to 40 h ablation and allowed 48 h of recovery showed very few cells labelled with β-gal (Fig. 3J,J′). The conclusion from these experiments is that the duplicated structures do not derive from cells of Sd lineage but from cells of the original notum.

The experiments using *hid* as pro-apoptotic agent yielded different results. After 40 h of treatment, the morphology of the Sd domain, wing pouch and hinge, remains normal, despite the presence of many Dcp-1-labelled cells (Fig. S2B). After 48 h of recovery the Dcp-1 label disappears and most of the discs present with near-normal morphology in the appendage region, suggesting they have regenerated the ablated territory. Moreover, lineage tracking of the ablated Sd domain with β-galactosidase label after 48 h of recovery indicates that the regenerated wing territory derives from cells of the original Sd domain (Fig. S2D,D′). This regeneration is visualised in adult flies that differentiate wing structures of variable size and near-normal pattern (Fig. S2E,F). These results reinforce previous observations indicating the strong regenerative capacity of wing cells.

The different results obtained with *UAS-rpr* and *UAS-hid* as pro-apoptotic factors most likely derive from their different cell killing capacities. *UAS-rpr* appears to be a very effective cell death inducer and essentially eliminates the Sd region. *UAS-hid* is less effective and allows the survival of a sufficient number of Sd cells that regenerate wing structures.

Development (2017) 144, 3946-3956 doi:10.1242/dev.155507

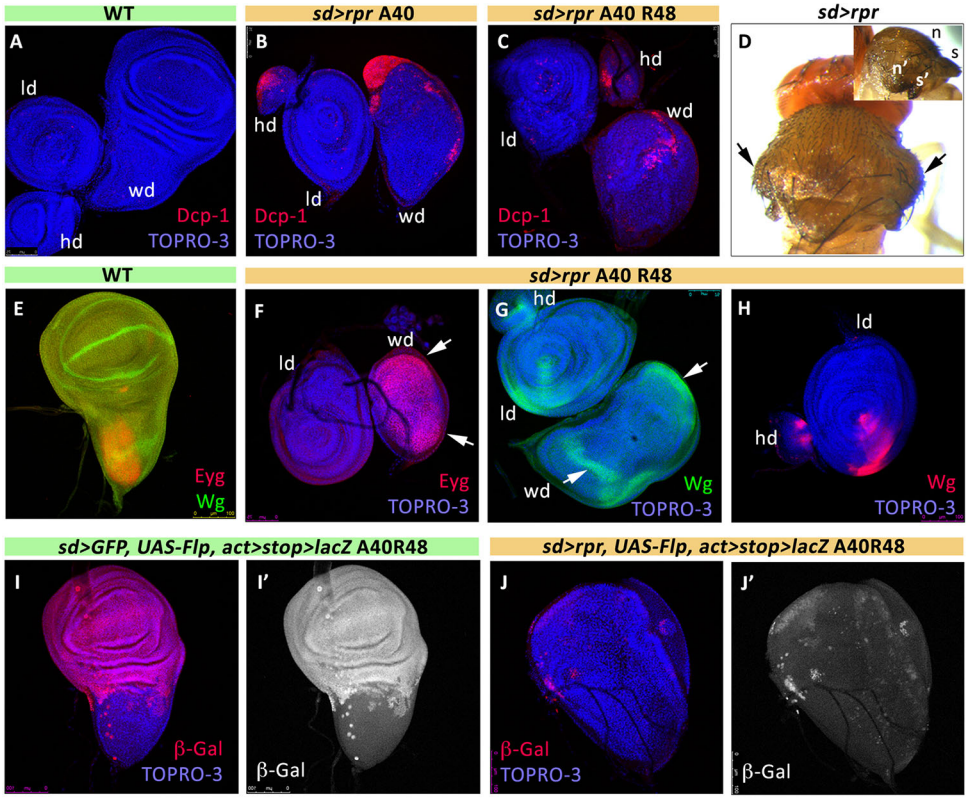

Fig. 3. Ablation of the Scalloped (Sd) domain. (A) Wild-type wing disc (wd), with a leg disc (ld) and a haltere disc (hd) in the vicinity. There is no Dcp-1 activity. (B) *sd>rpr* disc fixed immediately after 40 h of ablation. The disc has become very small (compare with control, A) and there is a strong Dcp-1 label in the region corresponding to the wing primordium (*n*=89). (C) Disc of the same genotype allowed 48 h of recovery after the ablation (*n*=74). There are still some dying cells labelled with Dcp-1. (D) An adult fly that emerged after 40 h of ablation (*n*=270 out of 300 flies). Note the lack of wing and the appearance of a notum duplicate (arrows). The inset shows the detail of the original notum (n) and scutellum (s), and the duplicated ones (n′,s′) of a different *sd>rpr* fly. (E-H) Distribution of Eyg (red) and Wg (green) proteins in wing and haltere discs allowed to recover for 48 h after the end of the ablation period. (E,F) Wild-type (E) and *sd>rpr* (F) wing disc showing Eyg staining covering the entire disc and in mirror-image, as indicated by the arrows (*n*=6). (G) *sd>rpr* wing disc showing duplication of the Wg stripe (white arrows) (*n*=20). (H) A haltere *sd>rpr* disc showing duplication of the Wg stripe (*n*=5). (I-J′) The results of the lineage-tracing experiments. In control discs (I,I′), the β-Gal labelling (red) marks the progeny of all the cells of the original Sd domain, which includes the hinge and the wing proper (*n*=14). In *sd>rpr* discs (J,J′), levels of the β-Gal label are very much reduced, indicating that the notum duplicates derive from original notum cells (*n*=19). A40 refers to discs fixed after 40 h of ablation and A40R48 refers to discs fixed 48 h after the end of the ablation.

The key observation from the preceding experiments is that after the complete elimination of the wing or the haltere primordium, the trunk (notum or metanotum) cells cannot regenerate the corresponding appendage. Instead, they form mirror-image duplicates of trunk structures. This is significant, as it suggests a limitation in the reprogramming of the trunk cells. In what follows, we have analysed developmental events associated with the appearance of these duplicates.

Proliferative response to the elimination of the appendage precursors: role of the JNK pathway

In the *sd>rpr* experiment, we measured the proliferative response to the elimination of the entire presumptive wing region. After 40 h of *rpr* activity, EdU levels are increased in cells close to the ablated tissue (Fig. 4B,B′, Fig. S3C and Fig. S4B,B″), identified by the high Dcp-1 levels. To check the possibility that some of the overproliferating cells are of hinge identity, we performed a double staining of EdU and the hinge marker Zinc finger homeodomain 2 (Zfh2) (Whitworth and Russell, 2003; Terriente et al., 2008). As illustrated in Fig. S4B-B″, the great majority of the over-proliferating cells do not express Zfh2, indicating that the duplicated nota derive from the original notum. This zone of high proliferation also shows elevated levels of *dMyc* (Fig. 4D,D′) and of the Yorkie targets *expanded-lacZ* (*ex-lacZ*) (Hamaratoglu et al., 2006) (Fig. 4F,F′) and *diap1-lacZ* (Huang et al., 2005) (Fig. 4H,H′). Similar observations were also made in homologous regions of the haltere disc (Fig. 4F,F′,H,H′).

As the ablation of the Pnr and Vein notum regions (Fig. 2 and Fig. S1) did not elicit a proliferative response, we surmised that the proliferative response in the notum cells of *sd>rpr* discs could be due to signals emanating from the dying wing cells. It is known that apoptotic cells secrete proliferative signals that may cause overgrowths and that the signalling process requires JNK activity (Ryoo et al., 2004; Pérez-Garijo et al., 2004, 2009). Consequently, we examined ablated *sd>rpr* wing discs for JNK activity, which in the wild type is restricted to the most-proximal region (Agnès et al., 1999).

To monitor JNK activity, we examined the levels of two well-known JNK targets: the metalloprotease 1 protein (Mmp1) (Srivastava et al., 2007; Stevens and Page-McCaw, 2012) and the *puckered* (*puc*) gene (Martín-Blanco et al., 2000). The results are illustrated in Fig. 5. In non-ablated discs, *puc* expression is restricted to some proximal cells (Fig. 5A,A′), but in ablated discs both *puc* expression and Mmp1 protein levels accumulate in Dcp-1-expressing cells (Fig. 5B,B′,D,D′), indicating upregulation of JNK in the dying wing cells.

To assay the functional connection between JNK activity in the dying cells and the increase of cell proliferation of their neighbours,

Development (2017) 144, 3946-3956 doi:10.1242/dev.155507

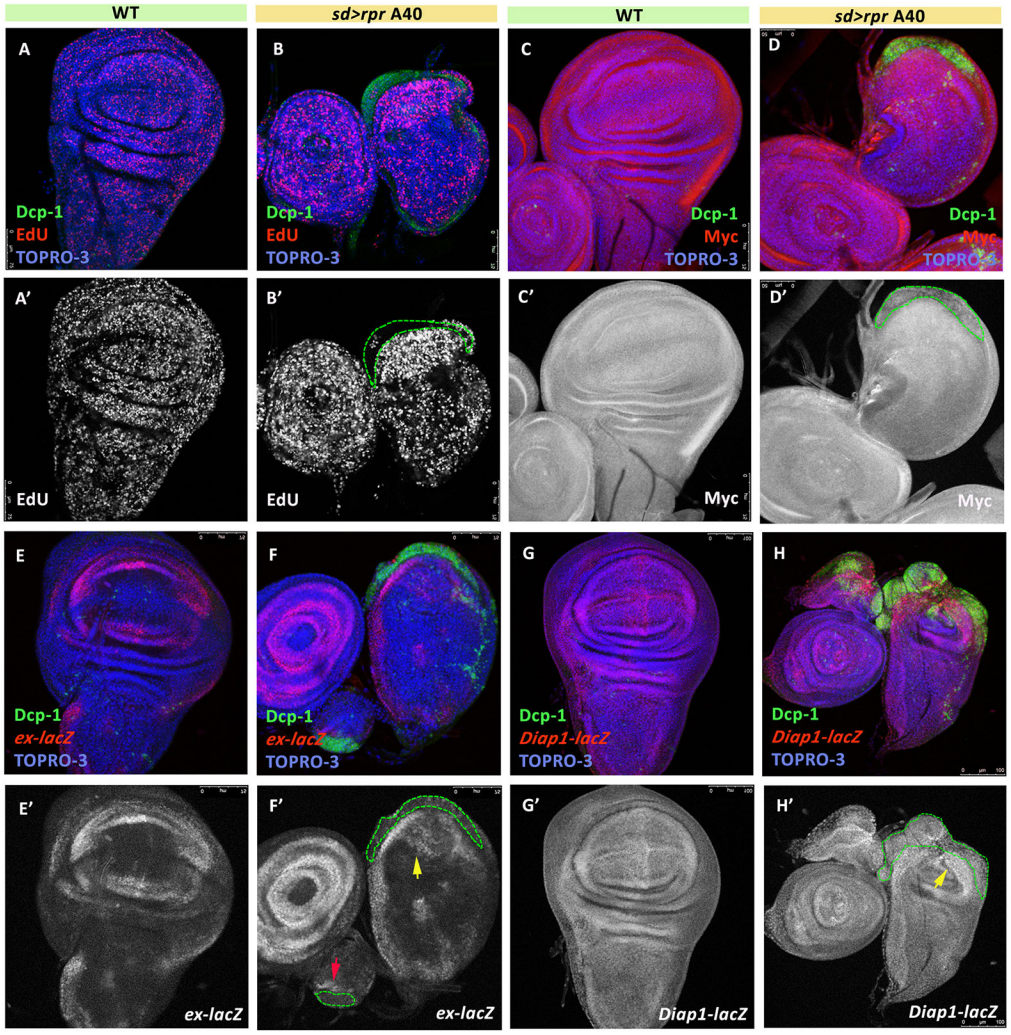

Fig. 4. Overproliferation of notum cells in the *sd>rpr* experiment. (A-B′) Comparison of the EdU incorporation (red) and apoptosis levels (Dcp-1, green) in control discs and *sd>rpr* discs after 40 h of ablation. In controls (A,A′), there is no apoptosis and EdU incorporation is uniform (*n*=17 discs). In *sd>rpr* discs (B,B′), there is strong Dcp-1 label in the few remaining wing cells (these do not incorporate EdU) and close to them there is a zone of intense EdU label (*n*=36 out of 38 discs). (C-D′) This area also presents high levels of Myc activity (red) (*n*=14). (E-H′) The augmented expression of the Yki targets *expanded* (*ex*) (F,F′) and *diap1* (H,H′) (arrows) in the zone of high proliferation close to the dying wing and haltere cells (*n*=11, 6). (E,E′) *ex-lacZ* and (G,G′) *Diap1-lacZ* in control discs. Green dashed lines delimit the ablated area labelled by Dcp-1. A40 refers to discs fixed after 40 h of ablation.

we compromised JNK activity in the ablated Sd domain by overexpressing *puc*, which functions as an inhibitor of the pathway (Martín-Blanco et al., 1998). In *sd>rpr UAS-puc* discs, cell proliferation levels in the proximity of the dying wing cells were reduced (Fig. 5F,F′) in comparison with those in *sd>rpr* discs in which JNK is functional (Fig. 5E,E′). We also observed that the inhibition of JNK results in reduction in the amount of tissue eliminated in the Sd domain. Although there is strong Dcp-1 label in the domain (Fig. 5F,F″), there are more cells surviving 40 h of *rpr* treatment. Our explanation for this difference is that inhibiting JNK interrupts the apoptosis amplification loop (Shlevkov and Morata, 2012), which results in lower apoptotic levels. This result illustrates the functional significance of the loop, which amplifies the strong apoptotic response generated by the *UAS-rpr* transgene.

Ablated *sd>rpr* and *sd>rpr UAS-puc* larvae can develop to adulthood; thus, we could compare their adult phenotypes. The results are shown in Fig. 5G: 87% of *sd>rpr* flies have duplicated nota compared with only 18% in *sd>rpr UAS-puc* flies. Interestingly, 45% of the latter show lack of wings but no notum duplication, and 37% are able to form some wing tissue.

The preceding results identify the JNK pathway as a principal factor responsible for the proliferative signalling originated in the wing cells in apoptosis. They also allow discrimination of the identity of signal-secreting cells (wing) and signal-responding cells (notum); notum cells respond to the signals emanating from dying wing cells. The fact that they cannot regenerate a wing but only form a duplicate of the notum suggests a restriction in the reprogramming capacity between notum (body trunk) and wing (appendage) structures.

The JNK pathway functions differently in the notum and in the wing

The proliferative response of the notum cells to JNK signalling emanating from dying wing cells contrasts with their lack of response to dying notum cells. We checked whether in the *pnr>rpr*, *248>rpr* and *vn>rpr* experiments JNK is activated after ablation in the notum regions and we found upregulation of Mmp1 and *puc-lacZ* in the corresponding notum domains (Fig. 6A-C′). These results show that the JNK pathway is activated in the notum in response to injury, but it appears incapable of inducing a proliferative response.

As JNK activity appears to have different effects in the notum and in the wing, we sought JNK targets that are expressed differentially after ablation. Recent work (Harris et al., 2016), has identified a *wg* enhancer (BRV118) in the wing disc that is specific to damage; within this enhancer the BRV-B module directs the strongest response. This fragment behaves as a target of JNK signalling and contains consensus sites that match the *Drosophila* AP-1 motif (Harris et al., 2016). We have compared the expression of the BRV-B module after ablation of the appendage cells (*sd>rpr* discs) and

Development (2017) 144, 3946-3956 doi:10.1242/dev.155507

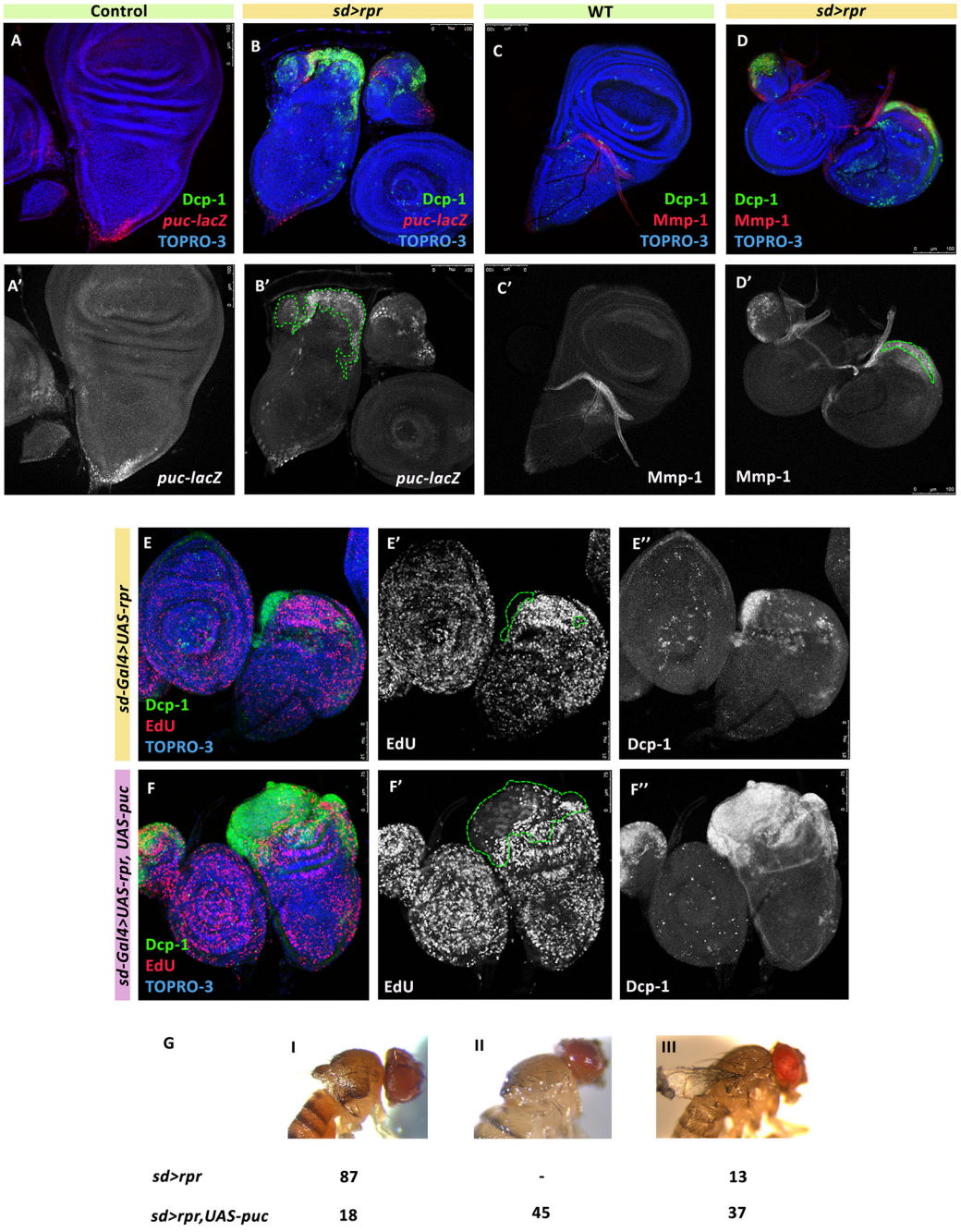

Fig. 5. JNK signalling is required to elicit a proliferative response after *rpr* ablation of the Sd domain. (A-D′) Confocal sections of control and *sd>rpr* ablated discs stained for the JNK targets *puckered* and Mmp1. In control discs (A,A′), *puc* expression (red) is restricted to a small proximal region of the disc, whereas in *sd>rpr* discs (B,B′), high *puc* levels are associated with dying wing cells, labelled green for Dcp-1 (n=8). The haltere disc is on the right, also showing Dcp-1 and *puc* expression in homologous regions. (C-D′) In control discs, Mmp1 (C,C′) is expressed in the trachea and the stalk, whereas in experimental discs (D,D′), Mmp1 appears close to the dying cells (n=16). The haltere disc (top left) shows a similar response. (E-F″) EdU incorporation in *sd>rpr* and *sd>rpr UAS-puc* experimental discs. In *sd>rpr* discs (E,E′), EdU levels (red) are locally increased in the region close to Dcp-1 cells (n=36 out of 38 discs). In *sd>rpr UAS-puc* discs (F,F′), the local increase of EdU is largely suppressed due to the inhibition of JNK activity. In addition, the amount of wing cells expressing Dcp-1 is significantly higher in these discs (F,F″) than in experimental *sd>rpr* discs (E,E″) (n=18 out of 20 discs). All staining was carried out at the end of the ablation period. (G) Percentage of *sd>rpr* (n=118) and *sd>rpr, UAS-puc* (n=104) adult flies showing the different phenotypes represented in the I, II and III photos. Green dashed lines delimit the apoptotic area.

after ablation of notum regions (*pnr>rpr*, *vein>rpr* and *248>rpr*). The results, illustrated in Fig. 6D-H′, indicate that although BRV-B is strongly expressed in the ablated wing region (Fig. 6H,H′), it is not induced in the ablated notum (Fig. 6E-G′).

The preceding experiments suggested that although the JNK pathway is induced upon ablation in the notum, the consequences are different from those observed in the wing. To explore the idea of differential function of JNK in different territories of the wing disc, we performed an experiment using the Gal4/UAS system to force constitutive activity of JNK in the Pnr domain of the notum and in the Spalt^{EPV} (Barrio and de Celis, 2004) domain of the wing. We have made use of the *UAS-hep^{CA}* transgene that induces high levels

Development (2017) 144, 3946-3956 doi:10.1242/dev.155507

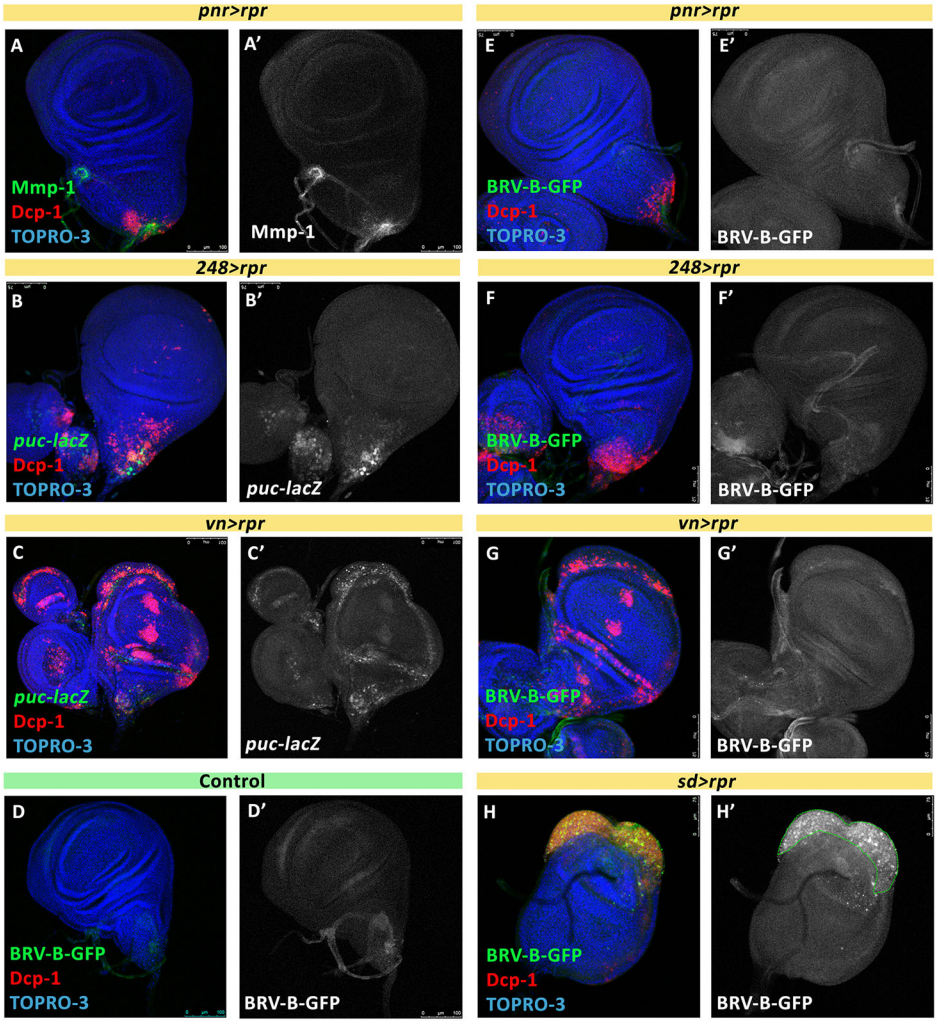

Fig. 6. Activation of JNK targets after ablation of the wing and the notum. (A-C′) Optical sections of *pnr>rpr*, *248>rpr* and *vn>rpr* ablated discs detecting Mmp-1 and *puc-lacZ* (*n*=18, 7, 18, respectively). (D-H′) BRV-B-GFP detection in control (D,D′), *pnr>rpr* (E,E′), *248>rpr* (F,F′), *vn>rpr*- (G,G′) and *sd>rpr* (H,H′) ablated discs (*n*=5, 29, 10, 12, 30, respectively). GFP is detected in the remaining damaged cells of the wing precursor in the *sd>rpr* experiment (H,H′), but not in ablated cells of the notum (E-G′). The BRV-B-GFP transgene is expressed at basal levels in the tracheas. All stainings were carried out at the end of the ablation period.

of constitutive JNK activity (Adachi-Yamada et al., 1999). Because one major property of JNK is to induce apoptosis (McEwen and Peifer, 2005; Igaki, 2009), the experiments were carried out in *dronc* mutant background so that affected cells cannot enter apoptosis (Xu et al., 2005). The results are illustrated in Fig. 7. We find that the overexpression of *hep* causes a large overgrowth in the Sal domain whereas it does not significantly affect the size of the Pnr domain (Fig. 7A-F). This increase in size is associated with upregulation of the Yki pathway, as indicated by the targets *expanded* and *cyclin E* (Fig. 7G-L′). This enlarged Sal domain also shows an increase in the proliferation levels, as indicated by the EdU levels (Fig. 7C). This distinct behaviour of JNK in notum and wing may be related to their different regeneration capacity.

Response to the ablation of trunk precursors

To study the response to the ablation of notum precursors, we used the *41D11-Gal4* line: an insertion at the *apterous* gene (Bieli et al., 2015) that drives expression in nearly all the notum and many hinge cells. Fig. 1D shows the expression of the line at the early larval third period, when we initiate ablation.

In discs fixed just after 40 h of ablation, we observe a clear diminution in the size of the disc, in particular in the notum region (Fig. 8B,B′), most of which is eliminated. There is also strong Dcp-1 label in this region and in the hinge. The loss of notum tissue is also visualised by the expression of Eyg, which becomes reduced to a small patch (Fig. 8D). In discs allowed to recover for 48 h after ablation, the notum region does not regenerate; it remains as a rudiment, as the Eyg label indicates (Fig. 8E). Interestingly, these discs show a large overgrowth of the zone close to the notum cells that alters their normal morphology (Fig. 8E). The position of the overgrown region suggested that it corresponds to hinge structures, as indicated by the expression of the hinge markers Stat (Bach et al., 2007; Ayala-Camargo et al., 2013) and Zfh2, expressed in the overgrown tissue (Fig. 8F-H). We cannot ascertain the identity of this tissue in cuticular structures because no adult flies emerge in this experiment.

The overgrowth of the hinge tissue is associated with an increase in proliferation in the corresponding zone of the disc, as indicated by the accumulation of EdU in the wing and haltere discs (Fig. 8I,I′). The two discs respond similarly to the ablation of the notum/hinge zone.

Following the observation in the *sd>rpr* experiment that JNK is responsible for the increased cell proliferation close to the ablated zone, we investigated the implication of the JNK pathway on the high proliferation levels observed in the hinge region in the 41D11 experiment. Indeed, staining for *puc-lacZ* indicates high JNK activity in the ablated region (Fig. 8J,J′). Moreover, the suppression of JNK in the zone, by overexpressing *puc*, results in almost suppression of the hinge overgrowths (Fig. 8K-L′). Furthermore, unlike the *41D11>rpr* experiment, some few *41D11>rpr, UAS-puc* flies emerge and differentiate wings that, although abnormal, show few signs of overgrowth.

Development (2017) 144, 3946-3956 doi:10.1242/dev.155507

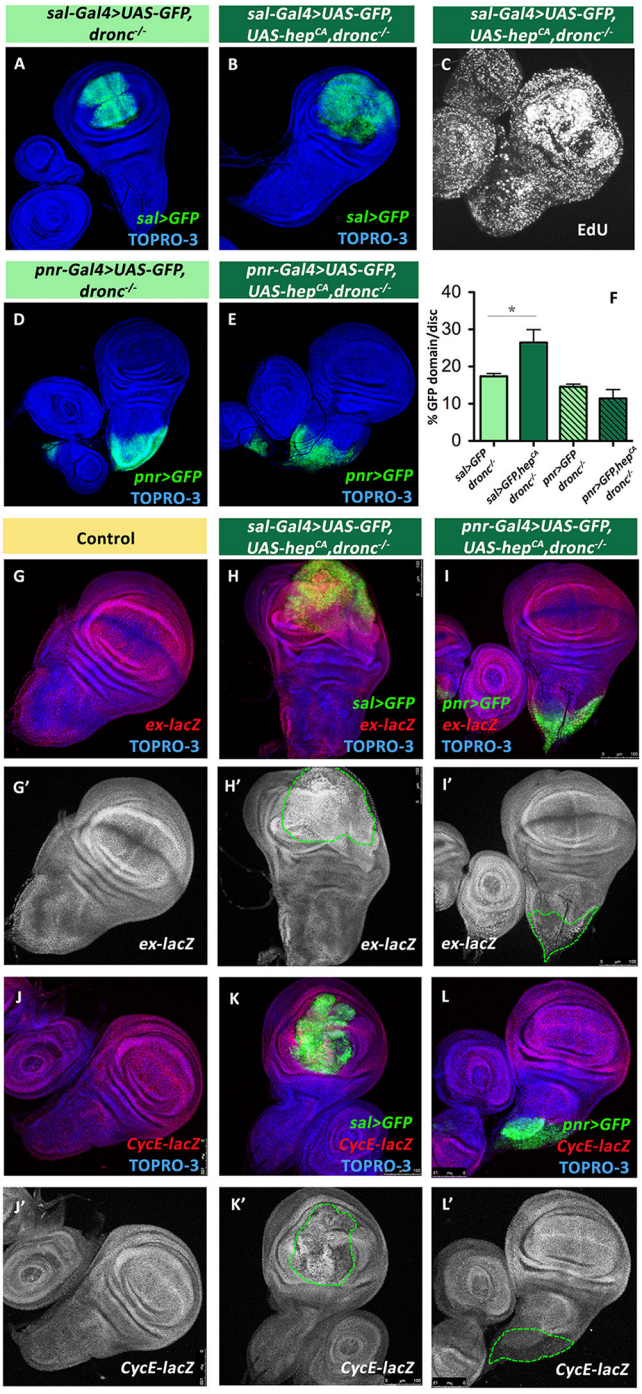

Fig. 7. Overexpression of JNK signalling in the wing and the notum. (A,D) The control Sal^{EPV} and Pnr domains (labelled by GFP) in *dronc*$^{I24/I29}$ discs. (B,E) The same Sal^{EPV} and Pnr domains in *dronc*$^{I24/I29}$ discs after 40 h of hep^{CA} activity. The Sal domain also exhibits high levels of EdU incorporation (C). (F) The percentage of the GFP area with respect to the total disc area in the genotypes *sal*^{EPV}*-Gal4, UAS-GFP,dronc*$^{I24/I29}$ (*n*=15); *sal*^{EPV}*-Gal4,UAS-GFP, UAS-hep*^{CA}*,dronc*$^{I24/I29}$ (*n*=14); *pnr-Gal4,UAS-GFP,dronc*$^{I24/I29}$ (*n*=9); and *pnr-Gal4,UAS-GFP,UAS-hep*^{CA}*,dronc*$^{I24/I29}$ (*n*=12). Data are mean±s.d.; **P*<0.0001. (G-L′) The expression of the Yki targets *ex-lacZ* and *CycE-lacZ* that are upregulated in the wing (H,H′,K,K′) (*n*=9, 13) but not in the notum (*n*=5, I,I′,L,L′) (*n*=6, 6) after 40 h of *hep*^{CA} activity.

This result reinforces the conclusion above that the increased cell proliferation triggered by ablation of the disc is mediated by activation of the JNK pathway in the dying cells. In this experiment, the ablated region includes notum and hinge cells, and because in the experiments ablating only notum there is no proliferative response, the additional cell proliferation observed here is most likely due to JNK activity in the hinge cells.

DISCUSSION

One major subdivision in the segmented body of *Drosophila* is that between body trunk and appendages, which is especially visible in the adult cuticle. In the case of the second thoracic segment, the dorsal cuticle is differentiated by the wing imaginal disc, which contains a trunk region (the notum) and an appendage, which includes the wing blade and associated hinge structures. The homologous haltere disc also contains a trunk region, metanotum and an appendage, the haltere. In this work, we have compared the regenerative potential of the different regions of those discs, with special attention to the distinction between trunk and appendage structures. The bulk of our results are based on the wing disc but we present evidence that the haltere disc behaves similarly.

Different regenerative potential of appendage and trunk regions

Classical transplantation experiments demonstrated the developmental plasticity of the imaginal discs (Hadorn and Buck, 1962; Nöthiger and Schubiger, 1966; Schubiger, 1971; Haynie and Bryant, 1976; reviewed by Worley et al., 2012), and recent reports using the Gal4/UAS/Gal80^{TS} method have confirmed the strong regenerative capacity of the wing disc (Smith-Bolton et al., 2009; Bergantiños et al., 2010; Sun and Irvine, 2011; Herrera et al., 2013). In addition, in our experiments forcing the pro-apoptotic gene *hid* in the Sd domain that covers the entire wing/hinge primordium, we find that the surviving wing/hinge cells are able to regenerate much of the lost wing tissue. Those experiments also identified genes and transduction pathways, *wg*, *dMyc*, Hippo pathway, JNK, etc., that appear to be associated with the regeneration process.

However, those studies paid very little attention to the trunk regions, one of the aspects we have explored in this work. One unexpected result is that the notum exhibits very limited regenerative potential. The ablation of the Pnr, Vein or 248 domains of the wing disc during the early third instar period leaves a permanent loss that cannot be recovered; the adult flies that emerge lack the corresponding structures (Fig. 2 and Fig. S1). This is in sharp contrast with the response of the wing regions, as mentioned above. The failure of the notum to regenerate matches the observation that, after the ablation of the Pnr and Vn domains, there is no detectable proliferative response in the neighbouring zones (Fig. 2, Fig. S1).

The finding that the notum and appendage respond differently to injury is novel and significant, for it describes a situation in which the same tissue, the wing imaginal disc (which cells originate from a common lineage), has developed two regions with very different regenerative potential. The study of the mechanism responsible for this difference may illuminate the distinct regeneration abilities found in diverse species of animals and in different tissues (Tanaka, 2003). We discuss this issue in connection with the function of the JNK pathway – see below.

The notum and wing/hinge territories appear to be developmentally isolated from each other

We have assayed the regenerative potential of the wing disc after ablation of the entire wing/hinge region – the *sd>rpr* experiments, or after ablating the entire notum territory, the *41D11>rpr* experiments. It is worth emphasising that, in our treatments using *rpr*, the targeted region is virtually eliminated

Development (2017) 144, 3946-3956 doi:10.1242/dev.155507

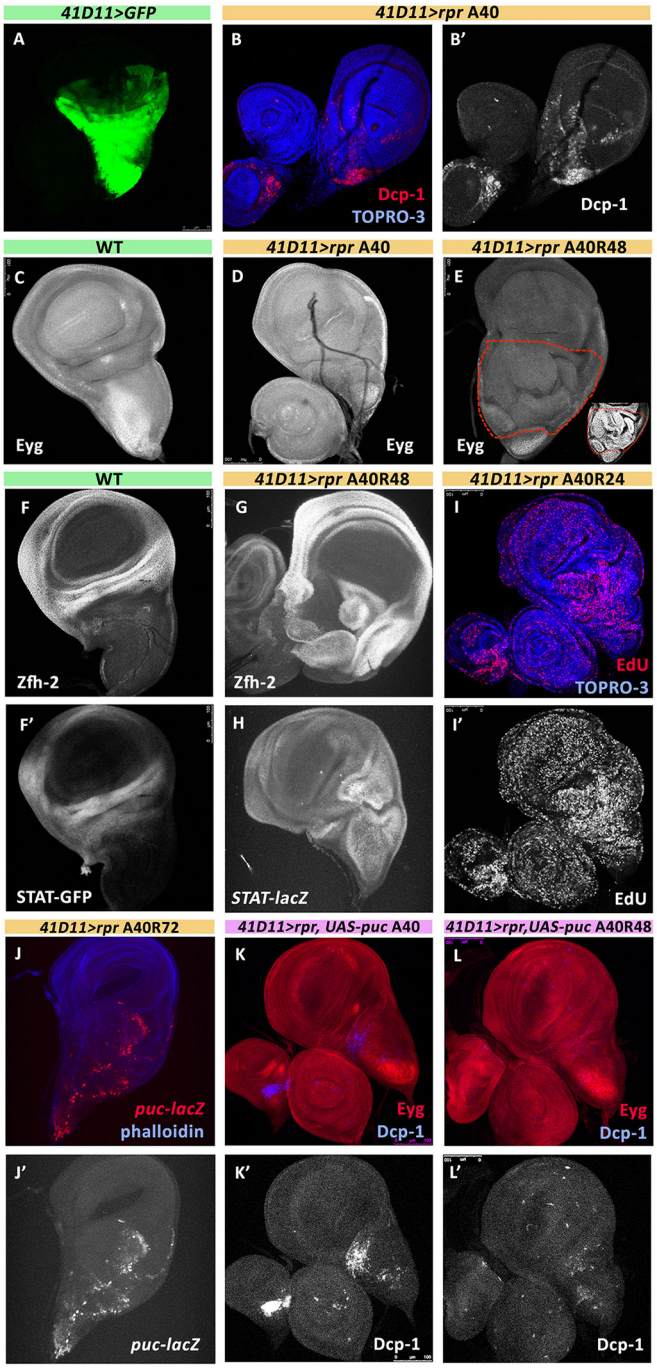

Fig. 8. Ablation of the entire notum (41D11 domain). (A) GFP marks the 41D11 region in a control disc. (B,B′) Dcp-1 protein levels in *41D11>rpr* discs at the end of the ablation period (n=16). (C-E) Eyg staining in wild-type (C) and *41D11>rpr* discs fixed 40 h after ablation (D) (n=8) and after 2 days of recovery (E) (n=19) shows the reduced notum region of ablated discs even after the recovery period. Dashed red line delimits the overgrown area observed in *41D11>rpr* ablated discs fixed after 2 days of recovery (E). Inset in E shows the extra folding of the overgrown tissue revealed by the TOPRO-3 staining. (F-H) Expression of the hinge markers Zfh-2 and STAT in wild-type (F,F′) and *41D11>rpr* ablated discs (G,H) (n=6, 4) fixed 2 days after recovery. (I,I′) EdU incorporation in ablated discs fixed after 24 h of recovery (n=17). (J,J′) Expression of *puc-lacZ* in *41D11>rpr* ablated discs fixed after 3 days of recovery (n=14). (K-L′) Eyg and Dcp-1 protein levels in *41D11>rpr* ablated discs overexpressing *puc* at the end of the ablation period (K,K′) (n=7) and after 2 days of recovery (L,L′) (n=8). A40 refers to discs fixed after 40 h of ablation and A40R48 refers to discs fixed 48 h after the end of the ablation.

(Figs 3 and 7). Thus, those experiments amount to a physical amputation.

The *sd>rpr* experiments yielded unexpected results: the cells close to the dying wing cells exhibit high proliferation levels, but they fail to regenerate the ablated wing/hinge structures and generate instead a notum duplicate. This is an intriguing observation, because it shows that, unlike in the Pnr, Vein and 248 experiments, notum cells can proliferate in response to injury (see below). The notum duplication can be visualised in mature discs after recovery (Fig. 3F,G), and is especially clear in the adult flies that emerge after the treatment, most of which show duplicated notum structures (Fig. 3D). The fact that notum cells in spite of their proliferative response can only develop notum structures is of interest, as it suggests that trunk cells cannot be reprogrammed to develop appendage structures. The fact that haltere discs from this experiment also produces metanotum duplicates (Fig. 3H) reinforces this latter point and makes it more general.

Notum duplications have been reported in classical transplantation experiments (Bryant, 1975), but the interpretation was very different. In those experiments, duplications were not limited to the notum; hinge and wing regions could also duplicate, depending on the size of the regenerating fragment; the behaviour of the fragments would depend on the positional values present in the fragment that would generate new positional values by the ‘shortest intercalation’ and the ‘complete circle’ rules (French et al., 1976).

The *41D11>rpr* experiment is complementary to the *sd>rpr* experiment. Here, the entire notum territory is eliminated and the wing/hinge cells respond to the injury. After ablation of the 41D11 domain, the notum territory is reduced to a minimum and does not regenerate, even after 48 or 72 h of recovery time (Fig. 7E). This failure to regenerate the notum contrasts with the increased cell proliferation in its vicinity. However, as shown by the molecular markers Stat and Zfh2, the overproliferating cells are mostly of hinge identity (Fig. 7G,H). Thus, the appendage cells cannot form notum structures, in spite of their proliferative response.

One general conclusion from these experiments is that both the notum and the wing primordia appear to be incapable of regenerating each other. The genetic programs specific to notum and wing become established during early larval period (Zecca and Struhl, 2002) from a pool of cells of common lineage. Our results clearly indicate that once the notum or the appendage program is established, it cannot be reversed, even after major injury to the disc. Additional observations of the haltere disc (Figs 3, 4 and 8) suggest that the irreversible trunk/appendage restriction is a general feature of the body.

The irreversibility of trunk/appendage identity even after massive damage is intriguing in view of our previous observation (Herrera and Morata, 2014) that anterior and posterior identity can be altered during regeneration: the trunk/appendage subdivision appears much later than the A/P subdivision and yet it is more rigid. We do not know the reasons for this difference, but it appears that the timing of the events is less crucial than the nature of the developmental decision.

The source of additional proliferation: role of the JNK pathway

The JNK pathway has been related with regeneration processes in *Drosophila* (Bosch et al., 2005; Bergantiños et al., 2010; Sun and Irvine, 2011; Repiso et al., 2011; Herrera et al., 2013; Herrera and Morata, 2014; Santabárbara-Ruiz et al., 2015) and also in planarian regeneration (Almuedo-Castillo et al., 2014). A relevant feature of JNK in *Drosophila* is that in many situations it promotes apoptosis (Igaki, 2009), and it is known that apoptotic cells generate

Development (2017) 144, 3946-3956 doi:10.1242/dev.155507

proliferative signalling (reviewed by Bergmann and Steller, 2010 and Morata et al., 2011), which in turn is mediated by JNK (Pérez-Garijo et al., 2009).

Our experiments here clearly establish the involvement of JNK in the additional cell proliferation caused by the ablation process in *Drosophila*. The notum duplications observed in the *sd>rpr* experiment and the hinge outgrowth in the *41D11>rpr* experiment are both associated with and dependant on upregulation of the JNK pathway in the cells in apoptosis. It is worth pointing out that, as clearly shown in the *sd>rpr* experiment, the JNK signalling is originated in the dying wing cells and received in the notum cells, which have different identity. These results highlight the relevant role of apoptosis in the regeneration phenomena.

The overproliferating cells exhibit upregulated expression of Yki targets such as *expanded* or *diap1* (Fig. 4), indicating downregulation of the Hippo pathway as the vehicle to induce high cell proliferation. The regulation of Hippo signalling by JNK during regeneration has been previously reported (Sun and Irvine, 2011, 2013).

One intriguing aspect of our findings is why the JNK pathway is unable to increase cell proliferation after ablation of notum regions such as the Pnr or Vein domains. This cannot be due to inability of notum cells to respond to proliferative signalling, as shown by the *sd>rpr* experiment where notum cells overproliferate. Nor is it due to lack of activation of JNK in the notum cells after ablation, as we show it is upregulated (Fig. 6A-C′). It is possible that JNK is activated in the notum at lower levels or that even if activated it cannot generate proliferative signalling. Along this line, we have observed that a JNK target, the BRV-B *wg* enhancer (Harris et al., 2016), is upregulated in wing cells upon ablation but not in notum cells, and a related observation has been reported in *eiger*-overexpressing clones (Harris et al., 2016). This already indicates a distinct response of trunk and appendage cells to JNK that may be reflected in their different abilities to induce cell proliferation. The proximal notum region contains resident JNK activity (Agnès et al., 1999) but it does not induce overproliferation.

Moreover, the experiments forcing the expression of JNK in the wing and the notum further support the notion of a differential response to JNK activity in notum and wing: the overexpression of JNK causes a large overgrowth in the Sal domain, correlated with upregulation of the Yki pathway. However, this effect is not observed in the Pnr domain (Fig. 7), which shows no increase in size. This distinct response exhibited by these two territories may be related to their different regeneration capacities.

MATERIALS AND METHODS

Drosophila strains

The *Drosophila* stocks used in this study were *sd-Gal4*, *pnr-Gal4* and *248-Gal4* (Calleja et al., 1996); *vn-Gal4* (Austin et al., 2014) and *41D11-Gal4* (Bieli et al., 2015); sal^{EPV}*-Gal4* (a gift from J. F. de Celis, CBMSO, Madrid, Spain); the BRV-B-GFP line (Harris et al., 2016); *tub-*$Gal80^{TS}$ (McGuire et al., 2003); *puc-lacZ* line (*puc*^{E69}) and *UAS-*puc^{14C} line (Martín-Blanco et al., 1998); *UAS-GFP* and *UAS-Flp* (BDSC); *act>stop>lacZ* (a gift from G. Struhl, Columbia University, USA); *ex-lacZ* (ex^{697}); *CycE-lacZ* (BDSC 10384) and *Diap-1-lacZ* ($Diap1^{j5C8}$); and *STAT-10xGFP* (Bach et al., 2007). STAT-lacZ; *UAS-rpr*, *UAS-hid* and *UAS-*hep^{CA}, lines are described in FlyBase. $dronc^{I24}$ and $dronc^{I29}$ are considered null alleles (Xu et al., 2005) and were provided by A. Bergmann (University of Massachusetts, USA).

Genetic ablation experiments and lineage tracing

The Gal4/UAS/$Gal80^{TS}$ system (Smith-Bolton et al., 2009) was used to induce the expression of the pro-apoptotic genes *rpr* or *hid* in the wing disc domains defined by the driver lines: *pnr-Gal4*, *vn-Gal4*, *248-Gal4*, *41D11-Gal4* and *sd-Gal4*. The expression of *rpr* or *hid* was temporally regulated by the thermo-sensitive $Gal80^{TS}$ inhibitor, which is active at 17°C and degraded at 29°C.

The standard protocol consisted of growing larvae at 17°C until day 7 after egg-laying (transition from 2nd to 3rd instar), except for the Vn experiments (in which larvae were grown at 17°C until day 6), and then shifting them to 29°C to allow for Gal4 function driving *rpr* or *hid* activity. After 40 h at 29°C, larvae were shifted back to 17°C to stop ablation and allow for recovery for an additional 48 h (Fig. 1I) or until the emergence as adult flies. In some experiments, the experimental larvae were kept at 29°C for the rest of development to allow continuous ablation of the targeted domain.

The *UAS-Flp, act>stop>lacZ* cassette was used to mark and track the progeny of the cells of the targeted domain. As previously described (Herrera et al., 2013), the *UAS-Flp* transgene becomes activated and produces large amounts of Flipase that recombine the *act>stop>lacZ* cassette. As a consequence, the great majority of cells in the target domain, and their progeny, are indelibly labelled by β-galactosidase activity.

Immunostaining

Immunostaining was performed as described previously (Shlevkov and Morata, 2012). Images were captured using a Leica DB5500 B confocal microscope.

The following primary antibodies were used: rabbit anti-Dcp1 (Cell Signaling, 9578), 1:200; mouse anti-β-galactosidase (DSHB 40-1a), 1:50; rabbit anti-β-galactosidase (Cappel, 55976), 1:2000; mouse anti-Wingless (DSHB 4D4), 1:50; mouse anti-Mmp-1 (DSHB, a combination of 3B8D12, 3A6B4 and 5H7B11), 1:50; guinea pig anti-Eyegone, 1:200 (a gift from N. Azpiazu, CBMSO, Madrid, Spain); mouse anti-Zfh2, 1:150 (gift of F. Diaz-Benjumea, CBMSO, Madrid, Spain); guinea pig anti-dMyc, 1:100 (in-house); and mouse anti-GFP (Roche, 11814460001), 1:200.

Fluorescently labelled secondary antibodies (Molecular Probes Alexa) were used at 1:200 dilution. TO-PRO3 (Invitrogen) was used at 1:600 dilution to label nuclei.

EdU incorporation

For EdU incorporation, wing imaginal discs were cultured in 1 ml of EdU labelling solution for 20 min at room temperature. Discs were washed once with 1× PBS and then fixed in 4% paraformaldehyde, 0.1% Triton for 1 h at room temperature. EdU detection was performed according to the manufacturer instructions (Click-iT EdU Alexa Fluor 555 Imaging Kit, ThermoFisher Scientific). Antibody labelling of the samples was performed after EdU detection following the immunostaining protocol described above.

Slide-mounting adult wings

Adult wings were mounted in Euparal Mounting medium after having dissected the flies in a mixture of alcohol/glycerine. Images were captured with a Leica microscope.

Quantitative analysis

Images were processed using the ImageJ software. In the hep^{CA} experiments, GFP-labelled area and total area of the discs were measured by using the Area Fraction option in set Measurements. In the *pnr>rpr* and *sd>rpr* experiments, the proliferation index was measured by calculating the ratio of the EdU-labelled area in two regions of the ablated discs. The number of discs analysed in each experiment is given in the figure legend. The *P*-values were calculated using the two-tailed Student's *t*-test.

Acknowledgements

We thank C. Estella for useful reagents and helpful suggestions, and I. Hariharan for fly stocks. We also thank R. González and A. Cantarero for technical support and E. Sánchez-Herrero for critical reading of the manuscript.

Competing interests

The authors declare no competing or financial interests.

Author contributions

Conceptualization: R.M., G.M.; Methodology: R.M., G.M.; Validation: R.M.; Formal analysis: R.M., N.P.; Investigation: R.M., N.P.; Resources: N.P.; Writing - original

draft: R.M., G.M.; Writing - review & editing: G.M.; Visualization: R.M., G.M.; Supervision: G.M.; Project administration: G.M.; Funding acquisition: G.M.

Funding

This work was supported by Ministerio de Economía y Competitivida [BFU2012-32397, BFU2013-50584-EXP and BFU2015-67839-P (MINECO-FEDER)].

Supplementary information

Supplementary information available online at
http://dev.biologists.org/lookup/doi/10.1242/dev.155507.supplemental

References

Adachi-Yamada, T., Fujimura-Kamada, K., Nishida, Y. and Matsumoto, K. (1999). Distortion of proximodistal information causes JNK-dependent apoptosis in *Drosophila* wing. *Nature* **400**, 166-169.

Agnès, F., Suzanne, M. and Noselli, S. (1999). The Drosophila JNK pathway controls the morphogenesis of imaginal discs during metamorphosis. *Development* **126**, 5453-5462.

Aldaz, S., Morata, G. and Azpiazu, N. (2003). The Pax-homeobox gene *eyegone* is involved in the subdivision of the thorax of Drosophila. *Development* **130**, 4473-4482.

Almuedo-Castillo, M., Crespo-Yanez, X., Seebeck, F., Bartscherer, K., Salò, E. and Adell, T. (2014). JNK controls the onset of mitosis in planarian stem cells and triggers apoptotic cell death required for regeneration and remodeling. *PLoS Genet.* **10**, e1004400.

Austin, C. L., Manivannan, S. N. and Simcox, A. (2014). TGF-α ligands can substitute for the neuregulin Vein in *Drosophila* development. *Development* **141**, 4110-4114.

Ayala-Camargo, A., Anderson, A. M., Amoyel, M., Rodrigues, A. B., Flaherty, M. S. and Bach, E. A. (2013). JAK/STAT signaling is required for hinge growth and patterning in the *Drosophila* wing disc. *Dev. Biol.* **382**, 413-426.

Bach, E. A., Ekas, L. A., Ayala-Camargo, A., Flaherty, M. S., Lee, H., Perrimon, N. and Baeg, G.-H. (2007). GFP reporters detect the activation of the Drosophila JAK/STAT pathway in vivo. *Gene Expr. Patterns* **7**, 323-331.

Barrio, R. and de Celis, J. F. (2004). Regulation of spalt expression in the *Drosophila* wing blade in response to the Decapentaplegic signaling pathway. *Proc. Natl. Acad. Sci. USA* **101**, 6021-6026.

Bergantiños, C., Corominas, M. and Serras, F. (2010). Cell death-induced regeneration in wing imaginal discs requires JNK signalling. *Development* **137**, 1169-1179.

Bergmann, A. and Steller, H. (2010). Apoptosis, stem cells and tissue regeneration. *Sci. Signal.* **3**, re8.

Bieli, D., Kanca, O., Requena, D., Hamaratoglu, F., Gohl, D., Schedl, P., Affolter, M., Slattery, M., Müller, M. and Estella, C. (2015). Establishment of a developmental compartment requires interactions between three synergistic cis-regulatory modules. *PLoS Genet.* **11**, e1005376.

Bosch, M., Serras, F., Martín-Blanco, E. and Baguñà, J. (2005). JNK signaling pathway required for wound healing in regenerating *Drosophila* wing imaginal discs. *Dev. Biol.* **280**, 73-86.

Bryant, P. J. (1975). Pattern formation in the imaginal wing disc of *Drosophila melanogaster*: fate map, regeneration and duplication. *J. Exp. Zool.* **193**, 49-77.

Calleja, M., Moreno, E., Pelaz, S. and Morata, G. (1996). Visualization of gene expression in living adult Drosophila. *Science* **274**, 252-255.

Calleja, M., Herranz, H., Estella, C., Casal, J., Lawrence, P., Simpson, P. and Morata, G. (2000). Generation of medial and lateral dorsal body domains by the pannier gene of Drosophila. *Development* **127**, 3971-3980.

French, V., Bryant, P. J. and Bryant, S. V. (1976). Pattern regulation in epimorphic fields. *Science* **193**, 969-981.

Hadorn, E. and Buck, D. (1962). On the differentiation of transplanted wing imaginal disc fragments of *Drosophila melanogaster*. *Rev. Suiss. Zool.* **69**, 302-310.

Hamaratoglu, F., Willecke, M., Kango-Singh, M., Nolo, R., Hyun, E., Tao, C., Jafar-Nejad, H. and Halder, G. (2006). The tumour-suppressor genes NF2/Merlin and Expanded act through Hippo signalling to regulate cell proliferation and apoptosis. *Nat. Cell Biol.* **8**, 27-36.

Harris, R. E., Setiawan, L., Saul, J. and Hariharan, I. K. (2016). Localized epigenetic silencing of a damage-activated WNT enhancer limits regeneration in mature Drosophila imaginal discs. *Elife* **3**, e11588.

Haynie, J. L. and Bryant, P. J. (1976). Intercalary regeneration in imaginal wing disk of Drosophila melanogaster. *Nature* **259**, 659-662.

Herrera, S. C. and Morata, G. (2014). Transgressions of compartment boundaries and cell reprogramming during regeneration in Drosophila. *Elife* **3**, e01831.

Herrera, S. C., Martín, R. and Morata, G. (2013). Tissue homeostasis in the wing disc of Drosophila melanogaster: immediate response to massive damage during development. *PLoS Genet.* **9**, e1003446.

Huang, J., Wu, S., Barrera, J., Matthews, K. and Pan, D. (2005). The Hippo signaling pathway coordinately regulates cell proliferation and apoptosis by inactivating Yorkie, the *Drosophila* homolog of YAP. *Cell* **122**, 421-434.

Igaki, T. (2009). Correcting developmental errors by apoptosis: lessons from Drosophila JNK signaling. *Apoptosis* **14**, 1021-1028.

Martín-Blanco, E., Gampel, A., Ring, J., Virdee, K., Kirov, N., Tolkovsky, A. M. and Martinez-Arias, A. (1998). puckered encodes a phosphatase that mediates a feedback loop regulating JNK activity during dorsal closure in Drosophila. *Genes Dev.* **12**, 557-570.

Martín-Blanco, E., Pastor-Pareja, J. C. and García-Bellido, A. (2000). JNK and decapentaplegic signaling control adhesiveness and cytoskeleton dynamics during thorax closure in Drosophila. *Proc. Natl. Acad. Sci. USA* **97**, 7888-7893.

McEwen, D. G. and Peifer, M. (2005). Puckered, a *Drosophila* MAPK phosphatase, ensures cell viability by antagonizing JNK-induced apoptosis. *Development* **132**, 3935-3946.

McGuire, S. E., Le, P. T., Osborn, A. J., Matsumoto, K. and Davis, R. L. (2003). Spatiotemporal rescue of memory dysfunction in Drosophila. *Science* **302**, 1765-1768.

Morata, G. and Lawrence, P. A. (1977). The development of *wingless*, a homeotic mutation of *Drosophila*. *Dev. Biol.* **56**, 227-240.

Morata, G. and Sanchez-Herrero, E. (1999). Patterning mechanisms in the body and the appendages of *Drosophila*. *Development* **126**, 2823-2828.

Morata, G., Shlevkov, E. and Pérez-Garijo, A. (2011). Mitogenic signaling from apoptotic cells in *Drosophila*. *Dev. Growth Diff.* **53**, 168-176.

Ng, M., Diaz-Benjumea, F. J., Vincent, J.-P., Wu, J. and Cohen, S. M. (1996). Specification of the wing by localized expression of wingless protein. *Nature* **381**, 316-318.

Nöthiger, R. and Schubiger, G. (1966). Developmental behaviour of fragments of symmetrical and asymmetrical imaginal discs of Drosophila melanogaster (Diptera). *J. Embr. Exp. Morphol.* **16**, 255-268.

Pérez-Garijo, A., Martín, F. A. and Morata, G. (2004). Caspase inhibition during apoptosis causes abnormal signalling and developmental aberrations in *Drosophila*. *Development* **131**, 5591-5598.

Pérez-Garijo, A., Shlevkov, E. and Morata, G. (2009). The role of Dpp and Wg in compensatory proliferation and in the formation of hyperplastic overgrowths caused by apoptotic cells in the *Drosophila* wing disc. *Development* **136**, 1169-1177.

Repiso, A., Bergantiños, C., Corominas, M. and Serras, F. (2011). Tissue repair and regeneration in Drosophila imaginal discs. *Dev. Growth Differ.* **53**, 177-185.

Ryoo, H. D., Gorenc, T. and Steller, H. (2004). Apoptotic cells can induce compensatory cell proliferation through the JNK and the Wingless signaling pathways. *Dev. Cell* **7**, 491-501.

Santabárbara-Ruiz, P., López-Santillán, M., Martínez-Rodríguez, I., Binagui-Casas, A., Pérez, L., Milán, M., Corominas, M. and Serras, F. (2015). ROS-induced JNK and p38 signaling is required for Unpaired Cytokine activation during Drosophila regeneration. *PLoS Genet.* **11**, e1005595.

Schubiger, G. (1971). Regeneration, duplication and transdetermination in fragments of the leg disc of *Drosophila melanogaster*. *Dev. Biol.* **26**, 277-295.

Shlevkov, E. and Morata, G. (2012). A dp53/JNK-dependant feedback amplification loop is essential for the apoptotic response to stress in Drosophila. *Cell Death Diff.* **19**, 451-460.

Smith-Bolton, R. K., Worley, M. I., Kanda, H. and Hariharan, I. K. (2009). Regenerative growth in Drosophila imaginal discs is regulated by Wingless and Myc. *Dev. Cell* **16**, 797-809.

Srivastava, A., Pastor-Pareja, J. C., Igaki, T., Pagliarini, R. and Xu, T. (2007). Basement membrane remodeling is essential for Drosophila disc eversion and tumor invasion. *Proc. Natl. Acad. Sci. USA* **104**, 2721-2726.

Stevens, L. J. and Page-McCaw, A. (2012). A secreted MMP is required for reepithelialization during wound healing. *Mol. Biol. Cell* **23**, 1068-1079.

Sun, G. and Irvine, K. D. (2011). Regulation of Hippo signaling by Jun Kinase signaling during compensatory cell proliferation and regeneration, and in neoplastic tumors. *Dev. Biol.* **350**, 139-151.

Sun, G. and Irvine, K. D. (2013). Ajuba family proteins link JNK to Hippo signaling. *Sci. Signal.* **6**, ra81.

Tanaka, E. M. (2003). Regeneration: if they can do it, why can't we? *Cell* **113**, 559-562.

Tanaka, E. M. and Reddien, P. W. (2011). The cellular basis for animal regeneration. *Dev. Cell* **21**, 172-185.

Terriente, J., Perea, D., Suzanne, M. and Díaz-Benjumea, F. J. (2008). The *Drosophila* gene zfh-2 is required to establish proximal-distal domains in the wing disc. *Dev. Biol.* **320**, 102-112.

Whitworth, A. J. and Russell, S. (2003). Temporally dynamic response to Wingless directs the sequential elaboration of the proximodistal axis of the Drosophila wing. *Dev. Biol.* **254**, 277-288.

Worley, M. I., Setiawan, L. and Hariharan, I. K. (2012). Regeneration and transdetermination in Drosophila imaginal discs. *Annu. Rev. Genet.* **46**, 289-310.

Xu, D., Li, Y., Arcaro, M., Lackey, M. and Bergmann, A. (2005). The CARD-carrying caspase Dronc is essential for most, but not all, developmental cell death in *Drosophila*. *Development* **132**, 2125-2134.

Zecca, M. and Struhl, G. (2002). Subdivision of the *Drosophila* wing imaginal disc by EGFR-mediated signaling. *Development* **129**, 1357-1368.

Supplementary Information

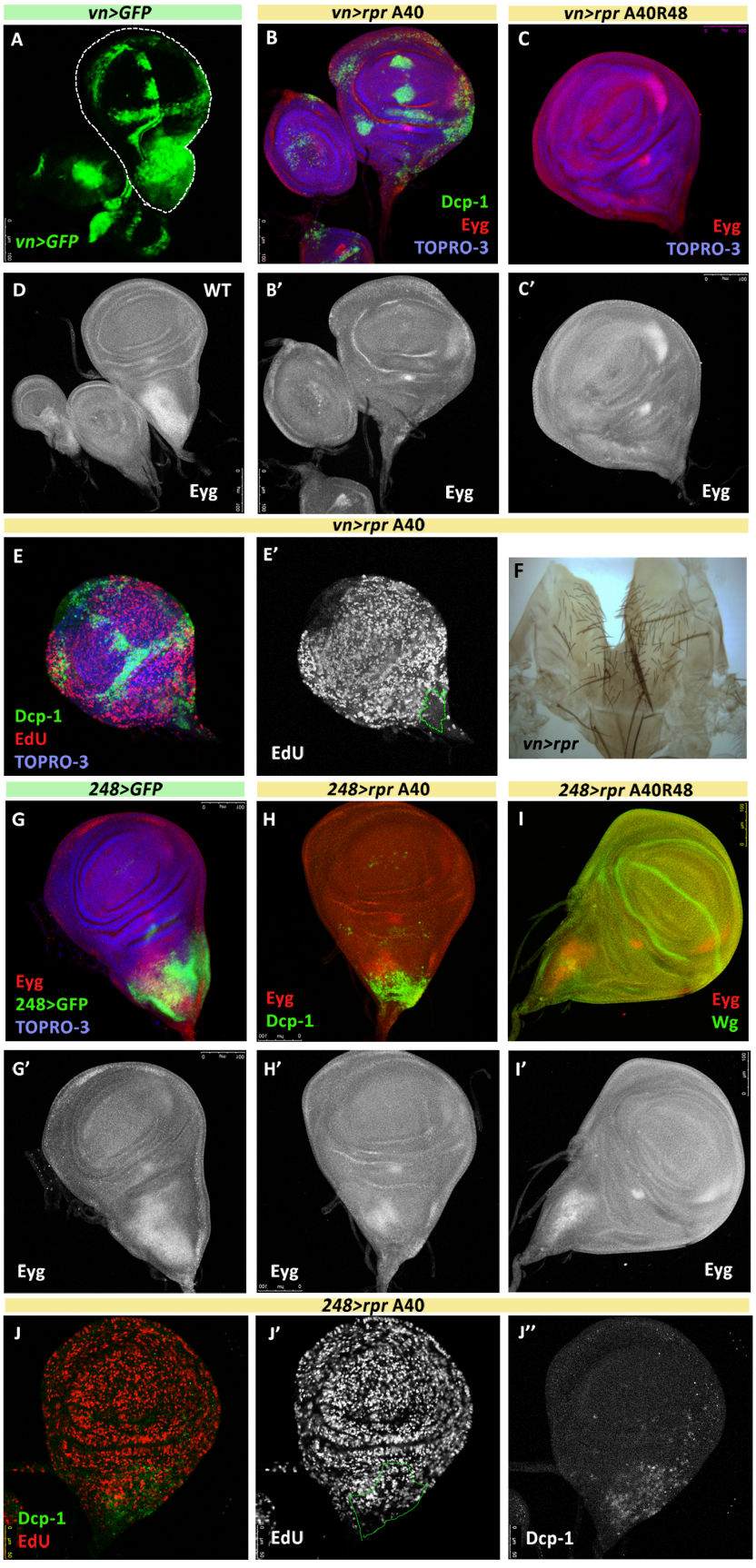

FIGURE S1

Figure S1. Ablation of the Vn and 248 domains. (A) GFP staining marks the Vn domain, which covers most of the notum and some cells of the hinge and the wing. (B, B') The absence of Eyg expression in the notum of ablated discs indicates that the notum region has been almost completely eliminated after 40 hrs of *rpr* expression. At the end of the ablation period, Dcp-1 levels are still detected in cells of the hinge and the wing (B). (C, C') The absence of Eyg label in the notum confirms that the ablated area has not been regenerated even after 48 hrs of recovery. (E, E') EdU incorporation is uniform in the wing disc, even in the cells close to the ablated area. The dashed green line delimits the ablated region of the notum. (F) Abnormal thorax of an adult fly emerging from *vn>rpr* larvae subjected to 40 hrs of ablation. Note that part of the lateral notum is missing compared to a WT fly (see Figure 2F). (G, G') GFP labels the domain in a control disc. The Eyg protein is visualized in red. (H, H') The significant reduction of Eyg levels in ablated discs indicates that a large part of the notum has been eliminated after 40 hrs of *rpr* expression in the 248 region. Dcp-1 is expressed in remaining dying cells of ablated discs. (I, I') The Eyg and Wg expression in ablated discs after 48 hrs of recovery suggests that regeneration of the 248 damaged area did not occurred after the recovery period. (J-J'') EdU incorporation in *248>rpr* ablated discs at the end of the ablation period.

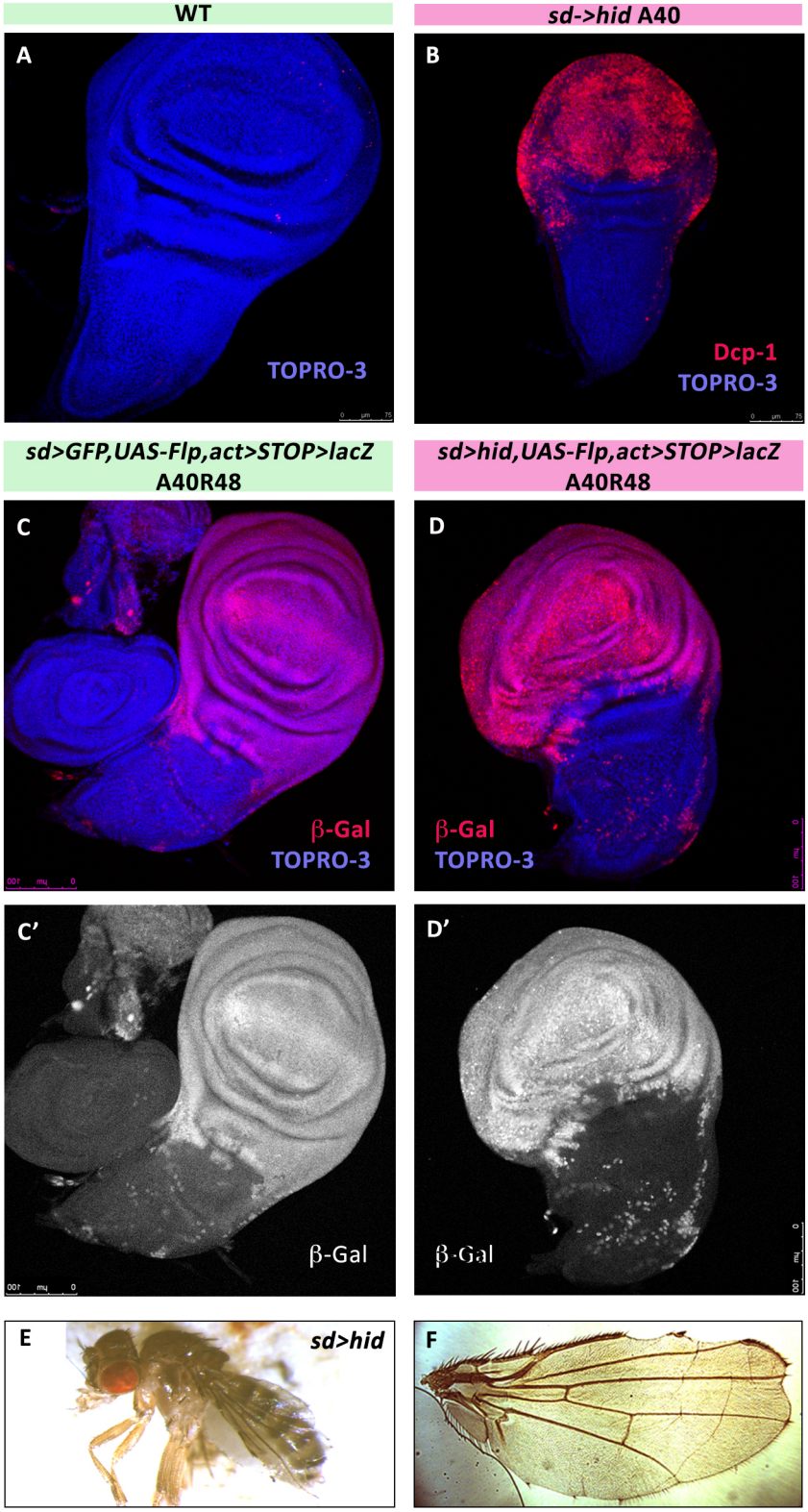

FIGURE S2

Figure S2. *hid*-induced ablation of the Sd domain. (B) Dcp-1 staining of *sd>hid* ablated disc which shows lots of cells undergoing apoptosis. The size of the ablated disc is smaller than the WT disc (A), although the general morphology is conserved after the ablation period. (C-D') Tracking of the progeny of ablated cells in *sd>GFP* and *sd>rpr* cells fixed after 2 days of recovery. (E) Adult fly emerging from a 40 hrs-ablated *sd>hid* larvae. (F) Detail of the wing of an experimental fly with identical genotype as the one shown in panel E.

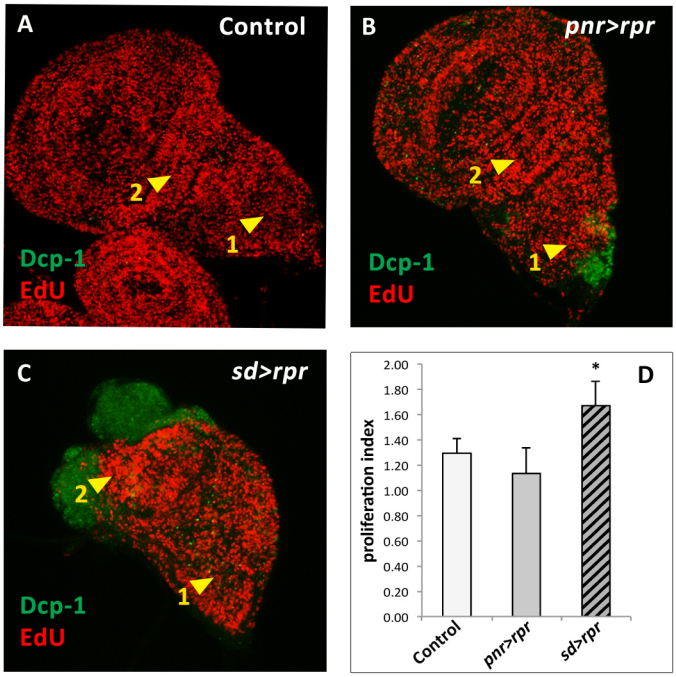

FIGURE S3

Figure S3. Quantification of the proliferation levels in the notum and the wing in response to ablation. Comparison of levels of EdU incorporation (red) in wildtype (A), *pnr>rpr* (B) and *sd>rpr* (C) discs. The region 1 in A, B, and C corresponds to the notum area, whereas the region 2 corresponds to a zone at the border between notum and wing appendage. Note that EdU incorporation levels in region 1 in are similar in wildtype (A) and *pnr>rpr* (B) discs, indicating that the ablation of the Pnr domain (green) does not significantly affect cell proliferation in the zone close to the ablated area. The disc in C shows augmented EdU label in region 2 in comparison with region 1. The area of high proliferation is adjacent to the ablated appendage. The histogram in D shows a quantification of the ratio of EdU incorporation of regions 2 and 1. Note the increased relative 2/1 EdU levels in *sd>rpr* discs (asterisk) with respect to control. (Control, n=2; *pnr>rpr*, n=8; *sd>rpr*, n=7 discs).

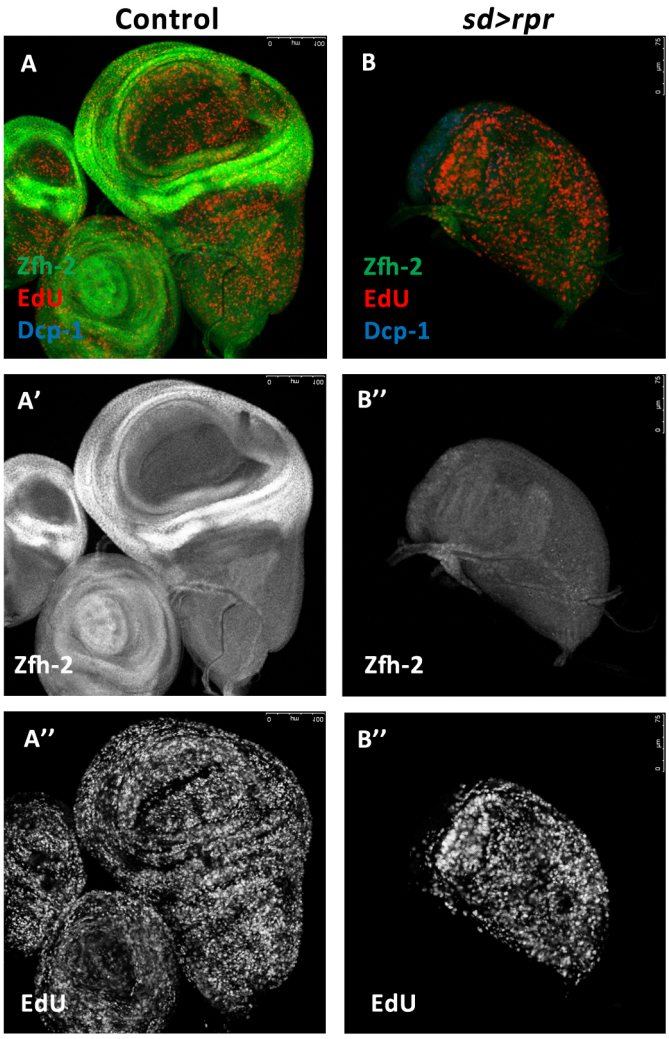

FIGURE S4

Figure S4. Identity of over-proliferating cells in *sd>rpr* discs.

EdU incorporation levels in control (A-A") and *sd>rpr* (B) discs. The expression of the marker Zfh2 (green) identifies cells of hinge identity, as indicated in A. In the *sd>rpr* (B-B") disc the area expressing Zfh2 is much diminished and mainly comprises dying cells. The over-proliferating cells, which contain higher EdU label (red), do not express Zfh2, indicating that they are not hinge but notum cells.